NONLINEAR OPTICAL PHENOMENA

PACS numbers: 42.55.Rz; 42.70.Hj
DOI: 10.1070/QE2005v035n10ABEH008994

Study of the phase component of an inverse population grating in a flashlamp-pumped Nd : $YAlO_3$ crystal

V.V. Tumorin, N.N. Il'ichev

***Abstract*. The relation between the phase and amplitude components of an inverse population grating in a Nd : $YAlO_3$ crystal is studied for different polarisations of probe radiation and under different conditions of flashlamp pumping. It is shown that temperature refractive-index gratings play a significant role in degenerate multiwave interactions in a saturated laser medium.**

Keywords: *Talbot effect, inverse population grating, solid-state lasers.*

1. Introduction

The development of a whole range of adaptive laser systems for phase conjugation (PC) of radiation upon degenerate four-wave mixing (DFWM) in a saturated laser medium [1 – 5] has lent a new impetus to the investigations of nonlinear resonance properties of laser materials. In many cases, lasing in a reciprocal loop resonator with a DFWM mirror [6 – 9] may be attributed to the phase component of an inverse population grating [10], recorded in the active laser medium under the action of superluminescent radiation.

The phase gratings of the refractive index variation can be produced not only due to the dependence of heat release on the degree of saturation of the laser medium [11 – 15], but also due to the difference in the polarisability of the activator ions in the ground and excited metastable states [16 – 19]. The ratio of the diffraction efficiencies of the amplitude and phase components of the inverse population gratings is described by the parameter [18, 19]

$$\beta = \frac{\chi_{\rm rl}}{\chi_{\rm im}} = \frac{k\delta n}{\delta\alpha}, \qquad (1)$$

where $\chi_{\rm rl}$ and $\chi_{\rm im}$ are the real and imaginary parts of the resonance susceptibility $\chi = \chi_{\rm rl} + {\rm i}\chi_{\rm im}$ of the laser medium, k is the wave number, and $\delta\alpha$ and δn are the variations in the field gain α and the refractive index n of the laser medium upon removal of inversion by the saturating radiation.

V.V. Tumorin, N.N. Il'ichev A.M. Prokhorov General Physics Institute, Russian Academy of Sciences, ul. Vavilova 38, 119991 Moscow, Russia; e-mail: ilichev@kapella.gpi.ru, vtumorin@kapella.gpi.ru

Received 4 May 2005; revision received 15 July 2005
Kvantovaya Elektronika **35** (10) 938 – 942 (2005)
Translated by Ram Wadhwa

A Nd : YAG crystal is the most widely used active medium of solid-state lasers with DFWM, which explains the growing interest in the investigations of nonlinear properties of this crystal. In earlier studies [16 – 18] of the electronic component of the refractive index of the Nd : YAG crystal, which varies under the action of the pump radiation, interference methods with probe beams of nonresonant radiation were employed. In some papers [17, 19 – 21], the degenerate and nondegenerate four-wave mixing technique was used for studying the phase component of a saturated gain grating. The results of these studies indicate that an increase in flashlamp pump power of the Nd : YAG crystal leads to a nonlinear increase in the parameter β, which may attain values 1.2 – 1.6 for $\alpha = 0.45$ cm^{-1}. The authors of these papers attribute the strong dependence of the refractive index of the Nd : YAG crystal on the inverse population density to the population of higher metastable levels of the 4f shell of the Nd^{3+} ion with a high polarisability, primarily of the highest $^2F(2)_{5/2}$ level with a lifetime of 3 μs.

An efficient population of this level from the $^4F_{3/2}$ metastable level occurs when the pump spectrum contains the UV components at wavelengths $\lambda < 330$ nm, which provide the transition to the levels of the 5d shell followed by nonradiative relaxation to the $^2F(2)_{5/2}$ level [22]. In the yttrium orthoaluminate ($YAlO_3$) matrix, the energy levels of the 5d shell of the Nd^{3+} ion lie above 52000 cm^{-1}, while the cross section of interconfigurational transitions is an order of magnitude smaller than in the Nd : YAG matrix [23]. The band gap between the 5d shell levels and the $^2F(2)_{5/2}$ level in Nd : $YAlO_3$ is 14000 cm^{-1}. Consequently, nonradiative multiphonon transitions between these levels are unlikely, and the levels in the 5d shell are depleted mainly due to luminescence. This is confirmed by a strong luminescence from the levels in the 5d shell observed in the region of wavelengths 370 – 420 nm upon pumping the Nd : $YAlO_3$ crystal by the harmonics of a neodymium laser [22]. In view of all that has been stated above, it can be assumed that the population of the $^2F(2)_{5/2}$ level in the flashlamp-pumped Nd : $YAlO_3$ crystal will occur with a lower efficiency than in the Nd : YAG crystal.

The drawback of the methods of measuring β with the help of probe beams at a nonresonant radiation frequency is the difficulty in the choice of a radiation source. For example, the probe radiation frequency in the case of a 0.633-μm He – Ne laser is close to the frequencies of transitions $^4I_{9/2} - {}^2H_{11/2}$ and $^4F_{3/2} - {}^4D_{1/2}$ ($^4D_{3/2}$, $^4D_{5/2}$, $^2L_{15/2}$) between the energy levels of the neodymium ion, which may lead to errors in determining the polarisability of

the excited states of neodymium ions at the resonance frequency.

We proposed a method [24] for determining the parameter β at the resonance frequency of probe radiation based on the self-reproduction of the radiation field in the near-field zone behind the grating (Talbot effect) [25]. The essence of the method lies in that if a plane monochromatic wave is incident on a 'thin' grating with period Λ, its image is reconstructed behind the grating at distances that are multiples of half the Talbot distance $Z_T/2 = \Lambda^2/\lambda$. The contrast of the interference pattern of the probe beam and the beams diffracted from the grating is a periodic function of the distance z from the grating with a period $Z_T/2$. For a sinusoidal amplitude–phase grating with a small modulation depth of transmission $T(x) \sim \exp[\Delta\alpha(1 - i\beta)\times \cos(2\pi x/\Lambda)]$, the maxima of contrasts are observed at distances $[(\arctan\beta)/\pi + m]Z_T/2$ from the grating, where m is an integer. Thus, knowing the shift of the curve showing the variation of contrast along the z axis relative to the position of the grating, we can determine the parameter β.

The complexity of this technique as applied to standard cylindrical crystalline active elements (AE) is that if the condition $Q = 2\pi\lambda L/(n\Lambda^2) \ll 1$ is satisfied for a 'thin' grating [26] (here, Q is the Klein parameter and L is the length of the AE), the contrast of the interference pattern is not restored due to the divergence of beams diffracted at the grating at a distance as small as $Z_T/2$. The interference pattern is found to be distorted due to diffraction of radiation at the AE aperture. Hence we used a telescope in our experiments to construct the image of the AE and considered the variation in the interference pattern contrast in front of the AE image as well as behind it. The parameter β was determined by the numerical simulation and fitting of the theoretical contrast variation curves with the experimental results.

The parameter β was determined in our experiments with an error of about ± 0.1, which is comparable with the values of β obtained for Nd : YAG. Hence, it is expedient to determine the dependence of the parameter β on the pump conditions by using a medium with a large β. For such a medium, we can choose Nd : $YAlO_3$ which is an anisotropic crystal with physical and lasing properties close to those of a Nd : YAG crystal. The cross section of laser transitions in Nd : $YAlO_3$ depends on the direction of propagation and polarisation of the radiation being amplified [27, 28]. The highest cross section corresponds to the transition at $\lambda = 1.0795$ μm during propagation of radiation along the b axis of the crystal with $\boldsymbol{E} \| c$. For the orthogonal polarisation ($\boldsymbol{E} \| a$), the cross section of the induced transition is just one-fourth of this value [27]. By assuming that the diffraction efficiency of the phase component of the inverse population grating depends weakly on the polarisation of the incident radiation, high values of the parameter β should be expected for the probe radiation polarisation corresponding to $\boldsymbol{E} \| a$.

2. Experimental setup

Figure 1 shows the scheme of the experimental setup. Active element (*4*) was a Nd : $YAlO_3$ crystal with a concentration of Nd^{3+} equal to 1 %. The AE had a size $\varnothing 6.3$ mm × 65 mm and was cut along the crystallographic axis b. The AE was excited by an INP-5/60 flashlamp in a K-301 quantron. The coolant was a 0.2 % aqueous solution of potassium dichromate. The inverse population grating in the AE was recorded upon a saturated gain of two intersecting beams from an external 1.0795-μm free-running Nd : $YAlO_3$ laser with a polarisation $\boldsymbol{E} \| c$. The interfering beams were formed upon reflection from the surface of glass wedges (*3*) separated by a distance of several tens of micrometers and arranged at an angle of about 0.54 mrad.

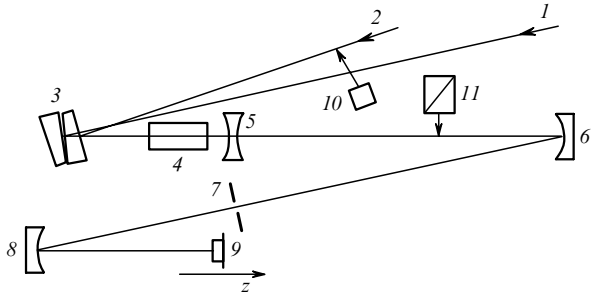

Figure 1. Experimental setup: (*1*, *2*) saturating and probe beams; (*3*) system of wedges; (*4*) Nd : $YAlO_3$ active element; (*5*) compensating negative concave lens; (*6*) reflector with a radius of curvature 2 m; (*7*) slit; (*8*) totally reflecting mirror with a radius of curvature 1.2 m; (*9*) CCD camera; (*10*) 90° quartz optical rotator; (*11*) Glan prism.

A part of the external laser radiation was used as the probe beam, which was reflected from the front surface of the system of wedges (*3*) and entered AE (*4*) at an angle of ~ 3 mrad to the plane of propagation of saturating beams. The projection of the direction of propagation of the probe beam on the plane of the saturating beams coincided with the bisector of the angle between them. The laser system worked with a pulse repetition rate of 2.5 Hz. Negative lens (*5*) with a focal length 7.5 m served to compensate for the thermal lens induced in AE (*4*). The image of AE (*4*) on CCD array (*9*) was obtained with the help of a telescope consisting of spherical reflector (*6*) with a radius of curvature 2 m, and totally reflecting mirror (*8*) with a radius of curvature 1.2 m. The video signal from the CCD array was digitised and fed to a computer. The CCD array was displaced along the z axis relative to the position of the image of AE (*4*), which led to a variation in the position of the objective plane of the telescope. Slit (*7*) with a variable gap was installed at the common focal plane of the telescope mirrors and was used for filtering lateral higher-order spatial diffraction peaks of the probe radiation at the gain grating. High-power saturating beams also overlapped in the region of slit (*7*).

The experiments were carried out for a constant energy 15 mJ of the saturating beams at the input to the amplifier. The energy of the probe beam was about 25 times lower. The polarisation of the probe radiation was changed from $\boldsymbol{E} \| c$ to $\boldsymbol{E} \| a$ by using quartz optical rotator (*10*). In the experiments with polarisation $\boldsymbol{E} \| a$ of the probe radiation, an additional polariser was installed behind AE (*4*) in the form of Glan prism (*11*) which extracted a powerful saturating radiation with polarisation $\boldsymbol{E} \| c$ from the system.

3. Experimental results

At the first stage, we measured the parameter β for the probe radiation polarisation $\boldsymbol{E} \| c$ using the method described in [24]. For the AE pump energy of 50 J, this parameter amounts to 0.13 ± 0.1, which is approximately in

accord with the value of β obtained by us earlier for Nd : YAG [24] under analogous experimental conditions.

A decrease in the diffraction efficiency of the amplitude gain grating as a result of variation of probe radiation polarisation to $\boldsymbol{E} \| a$ leads to a lowering of the maximum contrast of the interference pattern which is compatible with the nonuniformity of the transverse intensity distribution of the probe radiation caused by the diffraction at the AE aperture. This resulted in an increase in the error in determining the contrast of the interference pattern using the method described in [24].

In order to determine small values of the interference pattern contrast in this work, we recorded for each position of the CCD array on the z axis two images of transverse distribution of the intensity of probe radiation, one in the presence of an inverse population grating in the AE and the other without it (the saturating beams overlapped in front of the AE). The obtained intensity distributions over the transverse coordinate were normalised to the total intensity of the probe radiation for each image. The contrast of the interference pattern was determined as double the modulus of the Fourier component of the difference in normalised intensity distributions of the probe radiation at the grating spatial frequency:

$$K = 2\left|\int_{-\infty}^{\infty} [F(x) - F'(x)] \exp\left(\frac{2\pi i x}{\Lambda}\right) \mathrm{d}x\right|, \qquad (2)$$

where $F(x)$ and $F'(x)$ are the normalised transverse intensity distributions of the probe radiation with or without the saturated gain grating.

This method of determining the contrast of the interference pattern allows us to minimise the errors associated with the nonuniformity of transverse distribution of the probe radiation intensity. Figure 2 shows the variation of the contrast of the interference pattern, obtained by the method [24] used for probe radiation polarisation $\boldsymbol{E} \| c$ and proposed for the polarisation $\boldsymbol{E} \| a$. The distances along the z axis are recalculated for a beam in the region of the objective of the telescope comprised of mirrors (*6*) and (*8*). The position $z = 0$ corresponds to the central region of AE (*4*). The mathematical model described in [24] was used for processing the experimental data.

The values of the parameter β obtained for the probe radiation polarisation $\boldsymbol{E} \| a$ are 4.3 times larger than for the polarisation $\boldsymbol{E} \| c$, which is mainly in accord with the ratio of cross sections of induced transitions for orthogonal polarisations in Nd : $YAlO_3$. This means that the diffraction efficiency of the phase component of the inverse population grating in Nd : $YAlO_3$ depends weakly on the polarisation of the probe radiation. The absolute measuring error for the parameter β remains virtually unchanged in this case and amounts to ± 0.1, which makes it possible to study the dependence of β on the pump parameters.

The experiments carried out for pump energies of 25, 50 and 75 J showed a nearly linear dependence of the parameter β on the gain of saturating radiation (Fig. 3). The maximum variation of β was commensurate with the error in the measuring technique: the value of β increased from 0.48 ± 0.1 for $\alpha = 0.28$ cm^{-1} to 0.59 ± 0.1 for $\alpha = 0.47$ cm^{-1}. The dependence of the parameter β on the gain of the laser medium indicates that the emergence of the phase component of the inverse population grating is due not only to the difference in the polarisabilities of the levels $^4F_{3/2}$ and $^4I_{9/2}$ of the Nd^{3+} ion, but also to other factors.

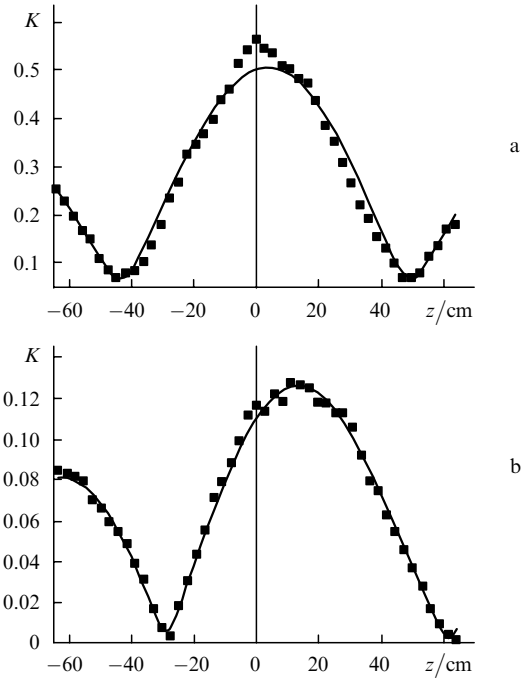

Figure 2. Variation of the contrast K along the z axis for probe radiation polarisation (a) $\boldsymbol{E} \| c$ and (b) $\boldsymbol{E} \| a$. The squares correspond to the experiment and the curves are calculations for $\beta = 0.13$ (a) and 0.56 (b).

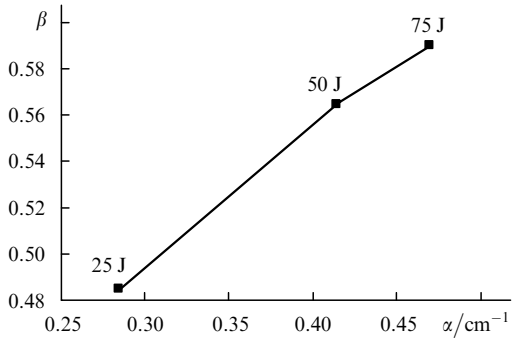

Figure 3. Dependence of the parameter β on the gain α upon varying the flashlamp energy.

In order to study the effect of the short-wavelength spectral region of pump radiation on the parameter β, we carried out an experiment in which Nd : $YAlO_3$ was placed in a quantron with a pure quartz monoblock. Distilled water was used as a coolant. It was found that for a probe radiation polarisation $\boldsymbol{E} \| a$ and a pump energy of 50 J, the parameter β was 0.34 ± 0.1, which is much smaller than the value $\beta = 0.56 \pm 0.1$ obtained by filtering the short-wavelength spectral region of the pump radiation.

The dependence of the parameter β on the pump radiation spectrum can be explained in a simple manner. It was mentioned above that the efficiency of population of the higher $^2F(2)_{5/2}$ level in Nd : $YAlO_3$ must be lower than in Nd : YAG due to a large band gap between the 4f and 5d shells. In this case, the refractive index of the laser medium may be influenced by the population of the $^2P_{3/2}$ level of the Nd^{3+} ion with the energy 26000 cm^{-1}, having a lifetime of 780 ns in Nd : $YAlO_3$ [29]. The pump bands for this level are located in the wavelength range 330–370 nm [30].

Our measurements of the pump radiation spectrum show that the short-wavelength component of the pump radiation with $\lambda < 430$ nm is efficiently absorbed in K-301 quantrons. Hence, the $^2P_{3/2}$ levels in such quantrons are efficiently populated only from the upper laser $^4F_{3/2}$ level. Recording of the inverse population grating in the laser medium leads to the emergence of a population grating for the higher level $^2P_{3/2}$ and hence to an increase in the amplitude of the refractive index variation grating. In the absence of filtration of the short-wavelength spectral region of the pump radiation, the efficiencies of populating the $^2P_{3/2}$ level from the ground state of the Nd^{3+} ion and from the upper laser level do not differ much, which leads to a decrease in the phase component of the inverse population grating.

The change in the pump radiation spectrum also affects the relation between the heat released during the absorption of pump radiation from the ground state of the Nd^{3+} ion and from the upper laser level. Filtration of the short-wavelength spectral region does not significantly change the heat released during absorption of the pump radiation from the upper laser level, since the absorption spectrum of the Nd^{3+} ion at $\lambda < 330$ nm contains only individual narrow absorption lines. On the contrary, the heat released due to absorption of pump radiation from the ground state depends strongly on the radiation intensity in this spectral region. Thus, filtration of the short-wavelength spectral region of the pump radiation lowers the relative heat release at the minima of the inverse population grating, which leads to an increase in the parameter β for a positive temperature dependence of the refractive index of the laser medium.

It must be mentioned that a significant radiation-induced colouring of the Nd : $YAlO_3$ crystal occurred during the experiment. However, repeated experiments with this AE in the K-301 quantron show that within the accuracy of the method, such a colouring of the crystal does not affect the parameter β.

The values of the parameter β obtained in our experiments are averaged over the period of action of free saturating and probe radiation from an external laser with a total duration of about 200 μs. Further information about the nature of the phase component of the inverse population grating can be obtained by studying the time dependence of the parameter β. Thus, the resonance component of the phase grating associated with the difference in the polarisabilities of the ground level and the upper laser level of Nd^{3+} ions is proportional to the amplitude component of the saturated gain grating. The phase grating formed due to population of the higher levels of the 4f shell from the upper laser level under the action of pump radiation depends not only on the population of the upper laser level, but also on the intensity of the flashlamp pump radiation.

The relaxation time τ_t of sinusoidal temperature gratings depends on the grating period Λ. For $\Lambda = 1$ mm, the relaxation time is $\tau_t = \Lambda^2/(4\pi^2\varkappa) \approx 5$ ms (where $\varkappa = 0.049$ $cm^2\ s^{-1}$ [31] is the thermal diffusivity of the $YAlO_3$ crystal), which is much longer than the lifetime of the upper laser level and hence the relaxation time of the inverse population grating. Thus, the temperature grating of the refractive index variation in our experiment may make a significant contribution to the phase component of the inverse population grating for long durations of interaction.

The time dependence of the parameter β was studied in an experiment in which the probe beam was provided by the single-mode radiation from an auxiliary passively Q-switched Nd : $YAlO_3$ crystal laser. The probe radiation polarisation in AE (*4*) was $\boldsymbol{E} \| a$. The contrast along the z axis was measured at various instants of the grating lifetime by varying the delay time between the pump pulses of the probe and saturating radiation generators. The experimental data were processed with the help of a simplified mathematical model using (unlike in [24]) a sinusoidal grating with distribution $\gamma(x) = (1 - i\beta)\Delta\gamma \cos^2(\pi x/\Lambda)$ of the gain increment along the transverse coordinate.

The obtained time dependences of the amplitude ($\Delta\gamma$) and phase ($\Delta\psi = \beta\Delta\gamma$) components of the grating, which are presented in Fig. 4, show that the phase component of the grating has a strong temperature component, whose lifetime is much longer than the lifetime of the inverse population grating. Due to the presence of this component, the parameter β increases monotonically with time and exceeds unity at $t > 300$ μs for radiation polarisation $\boldsymbol{E} \| a$. Thus, for a small angle of intersection of the beams being amplified and for a long interaction time, the temperature gratings of the refractive index variation may play a significant role in multiwave interactions in crystalline laser media. This conclusion agrees with the results of paper [32] in which the lasing threshold of a Nd : YAG holographic laser with a reciprocal loop cavity was studied as a function of the angle of intersection of the interacting beams.

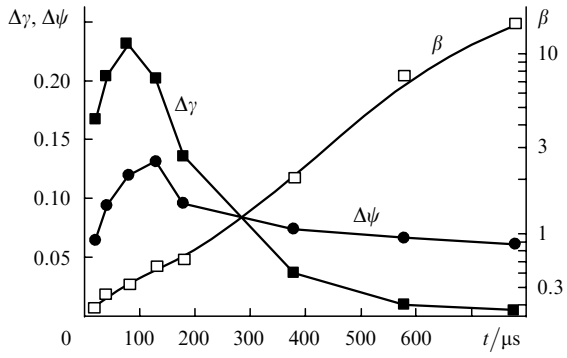

Figure 4. Time dependences of the amplitude ($\Delta\gamma$) and phase ($\Delta\psi$) components of the inverse population grating, and of the parameter β.

4. Conclusions

Our investigations of the relation between phase and amplitude components of the inverse population grating in Nd : $YAlO_3$ at the resonance frequency of radiation show that the anisotropy of the cross-section of induced transition in Nd : $YAlO_3$ is responsible for the dependence of the parameter β on polarisation of the probe radiation at 1.0795 μm. Under identical experimental conditions, the parameter β for orthogonal polarisations is equal to 0.13 ± 0.1 and 0.56 ± 0.1. This property of Nd : $YAlO_3$ makes it possible to enhance the relative accuracy of the method of measuring β which is based on the self-reproduction of the radiation field in the near-field zone behind the grating.

We have shown in our work that the parameter β depends on the flashlamp power. An increase in the gain of the medium from 0.28 to 0.47 cm^{-1} results in an increase in the parameter β from 0.48 to 0.59 for the polarisation

$E \| a$ of the probe radiation. The dependence of β on the intensity of flashlamp pump radiation in the short-wavelength spectral region was also detected. Measurements of the amplitude and phase components at various instants of the inverse population grating lifetime showed that for a small angle of intersection of the saturating radiation beams, the temperature gratings of refractive index variation may play a significant role in the processes of degenerate multiwave mixing in crystalline laser media.

Acknowledgements. This work was supported by the Russian Foundation for Basic Research (Grant No. 04-02-16059) and INTAS (Project No. 03-51-4893).

References

1. Damzen M.J., Green R.P.M., Syed K.S. *Opt. Lett.*, **20**, 1704 (1995).
2. Lam S.Y., Damzen M.J. *Appl. Phys. B*, **76**, 237 (2003).
3. Thompson B.A., Minassian A., Eason R.W., Damzen M.J. *Appl. Opt.*, **41**, 5638 (2002).
4. Sillard P., Brignon A., Huignard J.-P., Pocholle J.-P. *Opt. Lett.*, **23**, 1093 (1998).
5. Antipov O.L., Chausov D.V., Kuzhelev A.S., Vorob'ev V.A., Zinoviev A.P. *IEEE J. Quantum Electron.*, **37**, 716 (2001).
6. Bel'dyugin I.M., Berenberg V.A., Vasil'ev A.E., Mochalov I.V., Petrikova V.M., Petrovskii G.T., Kharchenko M.A., Shuvalov V.V. *Kvantovaya Elektron.*, **16**, 1142 (1989) [*Sov. J. Quantum Electron.*, **19**, 740 (1989)].
7. Antipov O.L., Kuzhelev A.S., Vorob'yov V.A., Zinov'ev A.P. *Opt. Commun.*, **152**, 313 (1998).
8. Pashinin P.P., Sidorin V.S., Tumorin V.V., Shklovskii E.I. *Kvantovaya Elektron.*, **24**, 57 (1997) [*Quantum Electron.*, **27**, 54 (1997)].
9. Basiev T.T., Fedin A.V., Gavrilov A.V., Smetanin S.N., Kyalbieva S.A. *Kvantovaya Elektron.*, **27**, 145 (1999) [*Quantum Electron.*, **29**, 140 (1999)].
10. Antipov O.L., Kuzhelev A.S., Chausov D.V. *Opt. Express*, **5** (12), 286 (1999).
11. Chen Y.F., Liao C.C., Lan Y.P., Wang S.C. *Appl. Phys. B*, **70**, 487 (2000).
12. Fluck R., Hermann M.R., Hackel L.A. *Appl. Phys. B*, **70**, 491 (2000).
13. Pollnau M., Hardman P.J., Kern M.A., Clarkson W.A., Hanna D.C. *Phys. Rev. B*, **58**, 16076 (1998).
14. Hardman P.J., Clarkson W.A., Friel G.J., Pollnau M., Hanna D.C. *IEEE J. Quantum Electron.*, **35**, 647 (1999).
15. Blows J.L., Omatsu T., Dawes J., Pask H., Tateda M. *IEEE Potonics Technology Lett.*, **10**, 1727 (1998).
16. Antipov O.L., Eremeykin O.N., Savikin A.P., Vorob'ev V.A., Bredukhin D.V., Kuznetsov M.S. *IEEE J. Quantum Electron.*, **39**, 647 (2003).
17. Antipov O.L., Kuzhelev A.S., Chausov D.V., Zinov'ev A.P. *J. Opt. Soc. Am. B*, **16**, 1072 (1999).
18. Antipov O.L., Kuzhelev A.S., Lukyanov A.Yu., Zinov'ev A.P. *Kvantovaya Elektron.*, **25**, 891 (1998) [*Quantum Electron.*, **28**, 867 (1998)].
19. Antipov O.L., Kuzhelev A.S., Chausov D.V. *Izv. Ros. Akad. Nauk, Ser. Fizich.*, **63**, 740 (1999).
20. Antipov O.L., Kuzhelev A.S., Chausov D.V. *Opt. Lett.*, **23**, 448 (1998).
21. Bufetova G.A., Nikolaev D.A., Shcherbakov I.A., Tsvetkov V.B. *Laser Phys.*, **13**, 245 (2003).
22. Antipov O.L., Ermeikin O.N., Savkin A.P. *Kvantovaya Elektron.*, **32**, 793 (2002) [*Quantum Electron.*, **32**, 793 (2002)].
23. Dubinskii M.A., Stolov A.L. *Fiz. Tverdogo Tela*, **27**, 2194 (1985).
24. Il'ichev N.N., Tumorin V.V. *Kvantovaya Elektron.*, **34**, 283 (2004) [*Quantum Electron.*, **34**, 283 (2004)].
25. Patorski K., in *Progress in Optics* (Amsterdam: Elsevier, 1989) Vol. 27, p. 3.
26. Klein W.R., Cook B.D. *IEEE Trans. Sonics Ultrason.*, **14**, 123 (1967).
27. Hanson F., Poirier P. *J. Opt. Soc. Am. B*, **12**, 1311 (1995).
28. Dischler B., Ennen H. *J. Appl. Phys.*, **60**, 376 (1986).
29. Basiev T.T., Dergachev A.Yu., Orlovskii Yu.V., Osiko V.V., Prokhorov A.M. *Trudy IOFRAN*, **46**, 3 (1994).
30. Weber M.J., Varitimos T.E. *J. Appl. Phys.*, **42**, 4996 (1971).
31. Penzkofer A. *Prog. Quantum Electron.*, **12**, 291 (1988).
32. Antipov O.L., Eremeykin O.N., Ievlev A.V., Savikin A.P. *Opt. Express*, **12**, 4313 (2004).